A consideration of the failure mechanism of river levees due to water seepage based on model tests and soil-water-air coupled finite deformation analysis

Un examen du mécanisme de rupture des digues fluviales en raison des infiltrations d'eaux à partir de tests sur modèles et d'analyse de déformation finie couplée sol-eau-air

Takahiro Yoshikawa
Department of Civil Engineering, Nagoya University, Japan, yoshikawa.takahiro@b.mbox.nagoya-u.ac.jp

Takeshi Kodaka, Ying Cui
Department of Civil Engineering, Meijo University, Japan

ABSTRACT: In most cases, overflow is taken as the main cause of failure of river levees due to heavy rain. As a result of recent damage in Japan, seepage failure has attracted considerable attention. To clarify the seepage failure mechanism of river levees, seepage model tests and a soil-water-air coupled finite deformation analysis of the tests were conducted. The SYS Cam-clay model was employed as an elasto-plastic constitutive model of the soil skeleton in the numerical analysis. From the numerical results, it was found that the analysis could simulate well the time and place of boiling phenomena, which shows the validity of the analysis. Furthermore, from case studies performed changing the permeability of the sandy layer directly below the levee or the seepage conditions, it was found that the arrangement of the two sand layers, the difference of the permeability between the layers, and the head difference significantly affected the occurrence of boiling and the deformation/failure patterns due to water seepage.

RÉSUMÉ: Dans la plupart des cas, le débordement est considéré comme la principale cause de défaillance des digues fluviales sous de fortes pluies. Suite à des dommages récents au Japon, les défaillances dues à l'infiltration ont attiré une attention considérable. Pour clarifier le mécanisme de défaillance des digues fluviales par infiltration, nous avons effectué des tests sur modèles et des analyses de déformation finie couplée sol-eau-air de ces tests. Dans l'analyse numérique, nous avons utilisé le modèle Cam-clay SYS comme modèle élasto-plastique constitutif du squelette du sol dans l'analyse numérique. À partir des résultats numériques, nous avons déterminé que l'analyse permettait une bonne simulation du temps et du lieu des phénomènes d'ébullition, ce qui montre la validité de l'analyse. En outre, à partir d'études de cas réalisées en modifiant la perméabilité de la couche sableuse située juste sous le niveau des conditions d'infiltration, nous avons constaté que l'agencement des deux couches de sable, la différence de perméabilité entre les couches et la différence de hauteur affectaient de manière significative la survenue des ébullitions et les motifs de déformation et de défaillance dues à l'infiltration d'eau.

KEYWORDS: Seepage failure, river levee, soil-water-air coupled finite deformation analysis, model test

1 INTRODUCTION

In Japan, where the duration of flooding is short, the main cause of collapse of river levees is overflow, and collapse due to seepage alone has not occurred for a long time. However, due to heavy rain in northern Kyushu in July 2012, failure of the Yabe River levee occurred, caused by local piping, and it was a great shock when river engineers and researchers realized that levees can collapse without overflow. It was reported that at the damaged location, a highly permeable layer that was directly connected to the river side below the clayey soil of the levee body was blocked (Yabe River Levee Study Committee 2013). In addition, regarding the Koyoshi River levee slope slip and the Kakehashi River slope failure that occurred in July 2013 (Document distributed at the special session concerning the damage report, Okado et al., 2014), it is considered that the damage was the result of highly permeable foundation ground. To date, river levees have been designed with emphasis on the shape of the cross section based on experience from damage in the past. Also, the standard method of analyzing the seepage slip failure of a levee body has been a combination of analysis methods, such as seepage flow analysis and circular slip surface analysis. However, levee failures caused by permeable foundation ground as described above have prompted the demand for the creation of new analysis methods based on the latest geotechnical mechanics to enable the rational and safe verification of river levees, taking into consideration complex ground conditions and hydraulic conditions.

In this research, seepage model tests and analysis using a soil-water-air coupled finite deformation analysis code (Noda and Yoshikawa 2015) were carried out with the objective of determining the mechanism of seepage failure of river levees on highly permeable foundations. This analysis code was developed by expanding a soil-water coupled finite deformation analysis code (Noda et al. 2008) to be capable of seamlessly handling unsaturated soil. These codes incorporate an elasto-plastic constitutive equation that is capable of describing the mechanical behavior of a wide range of soils within a uniform framework, the SYS Cam-clay model (Asaoka et al. 2002), and can handle deformation up to failure in a uniform framework for both static and dynamic external loads. This paper first describes seepage model tests having a blocked highly permeable layer. Next, simulation of the test was carried out to validate the analysis code, and it was shown that it is possible to reproduce well the seepage process and the location and timing of occurrence of boiling. In addition, case studies were carried out using the analysis code, from which the permeability and water level in the ground affected not only the occurrence of boiling but also the deformation mode in seepage failure.

2 OUTLINE OF SEEPAGE MODEL TEST AND ANALYSIS CONDITIONS

Figure 1 shows an outline of the seepage model test. In the test, water seeped from the right end of the model, and a layer of highly permeable Mikawa silica sand No. 3 was provided as the foundation. In order to represent the blockage of the highly

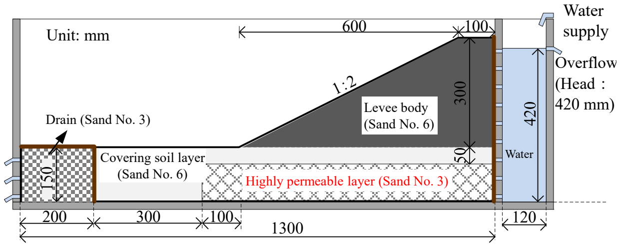

Figure 1. Outline of the seepage model test

Table 1. Saturated coefficient of water permeability for Mikawa silica sand Nos. 3, 6, and 8

		No. 3 sand	No. 6 sand	No. 8 sand
Saturated coefficient of water permeability m/s	k_s^w	4.06×10^{-3}	1.61×10^{-4}	2.21×10^{-5}

Table 2. Initial values used for the analysis

Constitutive equation of the soil skeleton, SYS Cam-clay model		
Degree of structure	$1/R^*_0$	4.0
Overconsolidation ratio	$1/R_0$	1.0
Void ratio	e_0	1.0
Stress ratio	η_0	0.545
Degree of anisotropy	ζ_0	0.545
Soil water characteristic		
Initial degree of saturation %	s_0^w	10.6

permeable layer that was reported at the damage location of the Yabe River levee, the Mikawa silica sand No. 3 layer was cut off part way. Mikawa silica sand No. 6 was used as the ground covering soil layer and the levee body. The detailed test results are described in the next section and compared with the analysis results.

The boundary conditions of the water and air in the analysis were as follows: a total head of 420 mm and unexhausted conditions at the right end where the water was seeping, undrained and unexhausted conditions at the bottom end, a seepage surface and unexhausted conditions at the left end water drainage part, and a seepage surface and exhausted conditions on the ground surface. The material constants for Mikawa silica sand No. 6 were determined by referring to Noda et al. (2008) for the constitutive equation of the soil skeleton, the SYS Cam-clay model and by referring to Sugii et al. (2002) for the soil water characteristic, the van Genuchten model (van Genuchten, 1980) and the Mualem model (Mualem 1976). For simplicity here, the difference between sand No. 3 and sand No. 6 was represented by changing the saturated coefficient of water permeability only. Table 1 shows the saturated coefficient of water permeability for Mikawa silica sand Nos. 3, 6, and 8. No. 8 sand was used as the covering soil layer in the case study described in Section 4 and has a lower permeability than No. 6 sand. The saturated coefficients of water permeability of No. 3 sand and No. 6 sand differ by a factor of about 20, and those of No. 3 sand and No. 8 sand differ by a factor of about 200. Table 2 shows the initial values used for the analysis. The initial state was defined in accordance with the test conditions. The initial specific volume, degree of structure, stress ratio, anisotropy, degree of saturation, pore air pressure (0 kPa), and pore water pressure (calculated from the soil water characteristic curve) were assumed to be constant within the ground. The overconsolidation ratio was distributed in accordance with the overburden pressure.

3 RESULTS OF SEEPAGE MODEL TESTS AND SIMULATION

Figures 2 and 3 show the results for the degree of saturation distribution in the seepage model test and the calculation results,

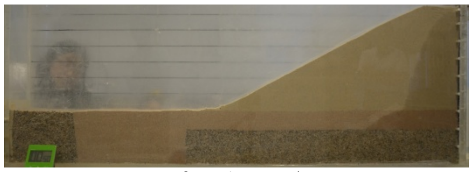

After 50 seconds

After 1 minute and 40 seconds

After 2 minutes and 20 seconds

After 4 minutes and 50 seconds

Figure 2. Seepage model test results

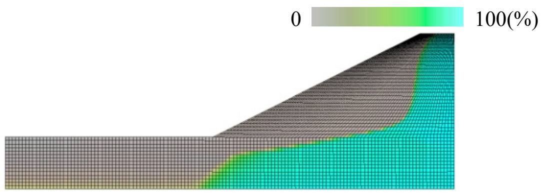

After 50 seconds

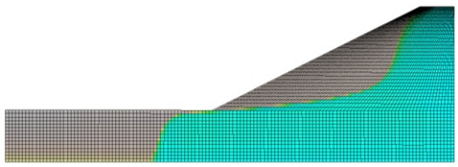

After 1 minute and 40 seconds

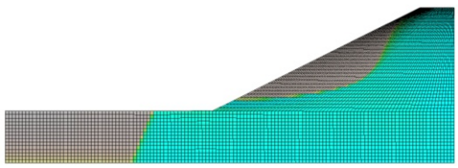

After 2 minutes and 20 seconds

Figure 3. Calculation results for distribution of degree of saturation

respectively. The calculation results reproduce well the permeation process of the test results. In the test, sand boiling occurred at 2 minutes and 20 seconds after the start of seepage at the location indicated by the red circle in the figure. As a result of this boiling, collapse occurred at 4 minutes and 50 seconds, with the levee body being reduced to about half its height. Figures 4 and 5 show the calculation results for the distribution of shear strain and mean skeleton stress (Jommi 2000), respectively. The calculation also shows that at 2 minutes and 20 seconds, the shear strain at the surface near the toe of the slope indicated by the red circle increased, and the mean skeleton stress reduced to near zero. The figures for these results are omitted due to space limitations, but as regards the

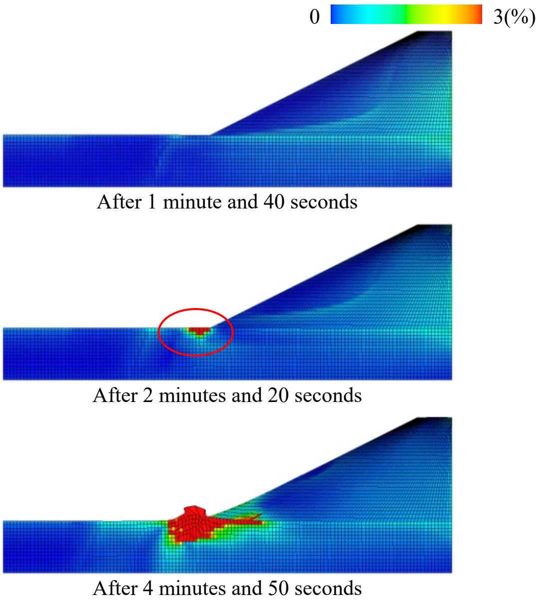

Figure 4. Calculation results for distribution of shear strain

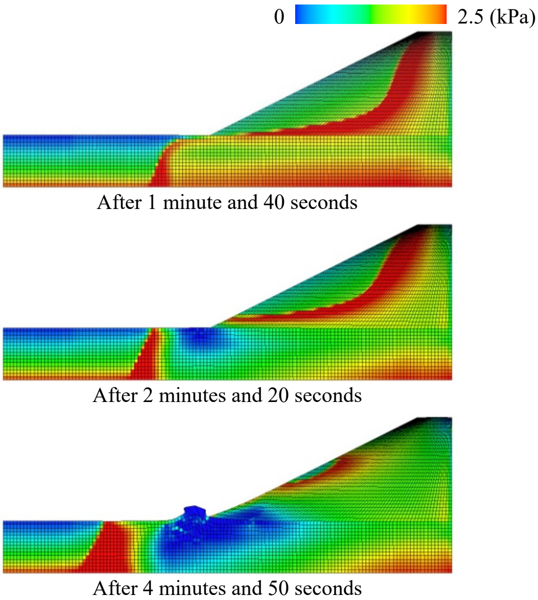

Figure 5. Calculation results for distribution of mean skeleton stress

mean skeleton stress-deviator stress relationship, softening behavior with plastic volume expansion is indicated above the critical state line. Thereafter, the deformation further increased at 4 minutes and 50 seconds, but at present, it is difficult to reproduce the collapse of the levee body as in the test.

From the above, it can be seen that the analysis code can reproduce well the process of occurrence of boiling phenomena due to seepage as the reduction of the skeleton stress associated with the increase in the pore water pressure.

4 CASE STUDIES (EFFECT OF SOIL PERMEABILITY AND WATER LEVEL ON THE OCCURRENCE OF BOILING)

The following 2 case studies were carried out by changing some of the analysis conditions of Section 3. The cases were as follows: (1) the covering soil layer in Figure 1 was given the saturated coefficient of water permeability of Mikawa silica sand No. 8, which has low water permeability, and (2) the conditions in (1) were changed by reducing the water level at the right end from 420 mm to 210 mm.

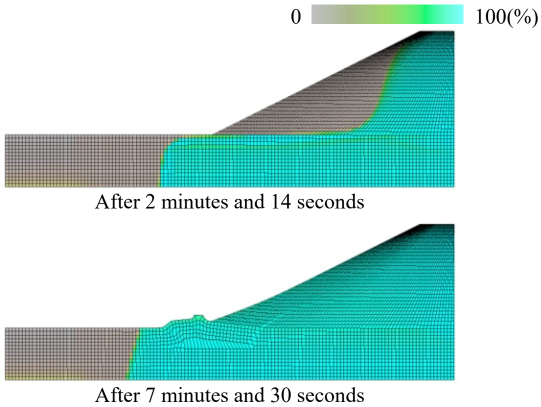

Figure 6. Calculation results for distribution of degree of saturation (the covering soil layer is No. 8 sand)

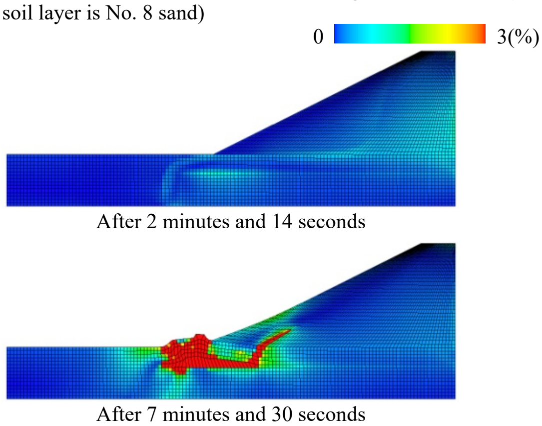

Figure 7. Calculation results for distribution of shear strain (the covering soil layer is No. 8 sand)

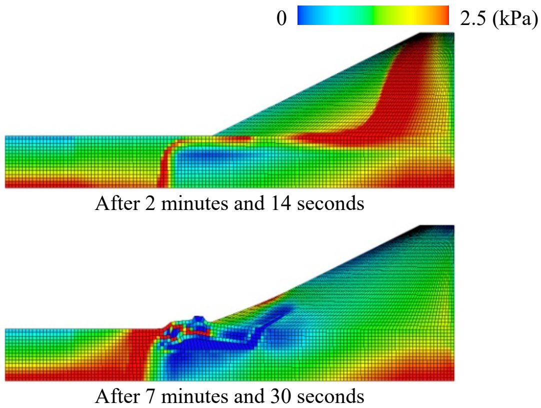

Figure 8. Calculation results for distribution of mean skeleton stress (the covering soil layer is No. 8 sand)

Figures 6 to 8 show the degree of saturation distribution, the shear strain distribution, and the mean skeleton stress distribution, respectively, for case (1), where the water permeability of the soil covering layer was low. Unlike the case in Section 3, when the phreatic surface extended past the highly permeable layer, the mean skeleton stress at the boundary between the layers approached zero, boiling with large shear deformation occurred, and the shear surface ultimately extended toward the levee body. Figures 9 to 11 show the degree of saturation distribution, the shear strain distribution, and the mean skeleton stress distribution, respectively, for case (2), where the water level only was changed to 210 mm from the conditions in (1). When the water level was reduced, the shear deformation was ultimately predominant at the ground surface, not at the boundary between the layers.

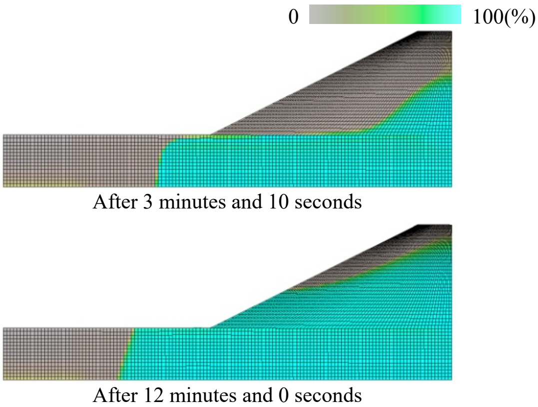

Figure 9. Calculation results for distribution of degree of saturation (the covering soil layer is No. 8 sand, and the water level is low at 210 mm)

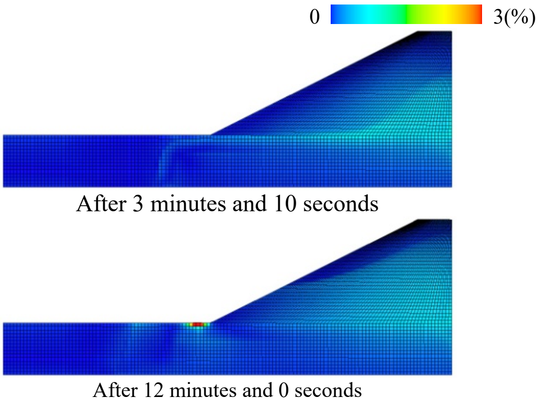

Figure 10. Calculation results for distribution of shear strain (the covering soil layer is No. 8 sand, and the water level is low at 210 mm)

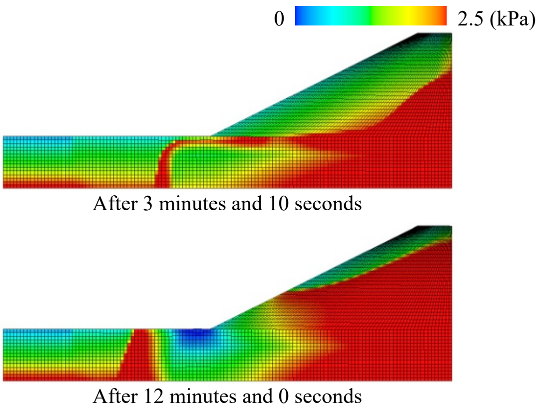

Figure 11. Calculation results for distribution of mean skeleton stress (the covering soil layer is No. 8 sand, and the water level is low at 210 mm)

From the above, it can be seen that differences in the water permeability of the soil layers and the external water level affect not only the occurrence of boiling failure but also the seepage failure mode.

5 CONCLUSION

By simulation of a seepage model test having a highly permeable layer, it was shown that the soil-water-air coupled elasto-plastic finite deformation analysis code (Noda and Yoshikawa 2015) can reproduce well the failure location and time as the boiling phenomenon of reduction of skeleton stress associated with an increase in pore water pressure (softening behavior with plastic volume expansion above the critical state line). Also, through the case studies, it was showed that differences in the water permeability of the soil layers and the external water level affect the amount of deformation and failure mode, in particular, in the case where the saturated coefficient of water permeability of the covering soil layer (2.21×10^{-5} m/s) was about 1/200th that of the highly permeable layer (4.06×10^{-3} m/s), boiling occurred at the boundary between the highly permeable layer and the covering soil layer, and the shear surface extended greatly toward the levee body.

With this analysis method, it is possible to evaluate the behavior of ground and soil structures within the same theoretical framework, regardless of the differences in soil material, target of evaluation, and form of external forces, such as whether the soil is sand or clay, the target is deformation or failure, or the external forces are rainwater or an earthquake. For the future, we are focused on evaluation from the hydraulic point of view, such as in the case of overflow of levees, etc., as well as evaluation by full-scale testing, and we wish to tackle problems regarding deformation and failure of river levees with a wide variety of soil materials and external forces including earthquakes.

6 ACKNOWLEDGEMENTS

This work was supported by JSPS KAKENHI Grant Number JP25249064 and the Ministry of Land, Infrastructure, Transport and Tourism's technical research and development for river levees. We had deep discussions with Prof. Noda of Nagoya University. The authors are grateful for these assistance.

7 REFERENCES

Yabe River Levee Study Committee: Report, Chikugo River Office, Kyushu Regional Development Bureau, 2013 (in Japanese).

Document distributed at the special session concerning the damage report, 2nd Symposium on Geotechnical Aspects of Levee Technology, Japan Society of Civil Engineers, 2014 (in Japanese).

Okado K., Iida D. and Imamori M.: Countermeasures against water leakage near Kobu on the Kakehashi River, 2014 Project Research Conference of the Hokuriku Regional Development Bureau, 2014 (in Japanese).

Noda, T. and Yoshikawa, T.: Soil-water-air coupled finite deformation analysis based on a rate-type equation of motion incorporating the SYS Cam-clay model, Soils and Foundations, 55(1), 45-62, 2015.

Asaoka, A., Noda, T., Yamada, E., Kaneda, K. and Nakano, M.: An elasto-plastic description of two distinct volume change mechanisms of soils, Soils and Foundations, 42(5), 47-57, 2002.

Noda, T., Asaoka, A. and Nakano, M.: Soil-water coupled finite deformation analysis based on a rate-type equation of motion incorporating the SYS Cam-clay model, Soils and Foundations, 48(6), 771-790, 2008.

Sugii T., Yamada K. and Okumura T.: Discussion of the unsaturated coefficient of water permeability of sand at high saturations, Abstracts of the 2001 Research Conference, Japan Society of Civil Engineers, Chubu Branch, 267-268, 2002 (in Japanese).

van Genuchten, M. T.: A closed-form equation for predicting the hydraulic conductivity of unsaturated soils, Soil Science Society of America Journal, 44, 892-898, 1980.

Mualem, Y.: A new model for predicting the hydraulic conductivity of unsaturated porous media, Water Resources Research, 12, 513-522, 1976.

Jommi, C.: Remarks on the constitutive modelling of unsaturated soils, Experimental Evidence and Theoretical Approaches in Unsaturated Soils (eds. by Tarantino, A. and Mancuso, C.), Balkema, 139-153, 2000.